

Geographical distribution and volume of Antarctic icebergs derived from ship observation data

Yury A. ROMANOV,¹ Nina A. ROMANOVA,¹ Peter ROMANOV²

¹*Shirshov Institute of Oceanology, 36, Nahimovski prospect, Moscow 117997, Russia.*

E-mail: romanov@ocean.ru

²*City College of City University of New York, 160 Convent Ave, New York, NY 10031, USA*

ABSTRACT. Information on the occurrence, spatial distribution and morphometric characteristics of Antarctic icebergs is needed in a large number of applications including navigation, heat and freshwater balance calculations, biochemistry of the ocean and climatology. Using over 60 000 ship observations of icebergs in the Southern Ocean collected since the end of the 1940s we have produced a detailed map of the distribution of Antarctic icebergs as well as maps of related statistics including the standard deviation, minimum and maximum values of the iceberg concentration and the probability of iceberg-free observations. The study incorporated small and medium-sized icebergs with a length of <10 nautical miles. Most observations were taken during the warm period of the year, from December to April. It is shown that the iceberg distribution across the Southern Ocean is determined by the location of calving regions and peculiarities of the atmospheric circulation and ocean currents. Iceberg concentration data combined with information on the iceberg size and shape distribution have been used to evaluate the area-integrated characteristics of Antarctic icebergs. The instantaneous number of icebergs in the Southern Ocean was estimated as 132 269 with an uncertainty of 7%. The area and volume of icebergs were equal correspondingly to 55 805 km² and 16 893 km³ with uncertainties of 32–33%.

KEYWORDS: Antarctic glaciology, calving, icebergs

INTRODUCTION

Icebergs present an intrinsic element of Antarctic waters. They are defined as massive floating bodies of freshwater ice whose height above the water level (or freeboard), length and width exceed correspondingly 5, 15 and 10 m. (WMO, 1970; Borodachev and others, 1994). Icebergs of different shape and size are formed through calving off ice shelves and outlet glaciers, as well as from the continental ice barrier (Shilnikov, 1969). Drifting in the Antarctic waters, overturning and gradually decaying along the way, icebergs can sometimes reach 43° S latitude in the Southern Atlantic and 50° S latitude in the Indian and Pacific Ocean (Romanov, 1996a, b). Icebergs affect navigation safety (Romanov, 1996b), control to a large extent, stratification and biochemical reactions in the waters of the Southern Ocean (Schwartz and Schodlock, 2009; Smith, 2011), and participate in the transfer of terrigenous material from the mainland to the ocean (Matsumoto, 1996; Licitzin, 2012). They are also an important source of fresh water (Weeks and Campbell, 1973; Spandonide, 2012) and can be used as tracers to characterize the water circulation (Radikevich and Romanov, 1995). With their bottom parts icebergs plow through or scour soft sediments of the seabed and therefore affect the lives of benthic communities and the bottom geomorphology (Gutt and Starmang, 2001; Dowdeswell and Bamber, 2007). When grounded in shallow waters, large icebergs can block the path of drifting ice and thus cause a radical change in the hydrological and hydro-biological environment (e.g., Arrigo and van Dijken, 2003). Other active areas of iceberg research include, but are not limited to mechanisms of the iceberg formation and decay (Provorkin, 1996; Massom, 2003; Wesche and others, 2013), the physical structure of icebergs (Popov and Voevodin, 1996) and their dynamics.

Giant icebergs with a size of over 10 nautical miles, nm (or 18.5 km) are routinely tracked by the National Ice Center, NIC (Ballantyne, 2002; Ballantyne and Long, 2002). Since 1979, icebergs with a size of over 5–6 nm have been monitored at Brigham Young University (Reeves and others, 2009). Calving of giant icebergs with a size of more than several nautical miles is relatively rare: only a few giant icebergs are produced per year by Antarctic glaciers and ice sheets. Information on the location and on the drift of giant icebergs is primarily obtained with satellite-based scatterometers as well as from moderate and high spatial resolution satellite optical imagery. Collected data on the large iceberg distribution and morphology derived from these observations have been summarized by Silva and others (2006) and Tournadre and others (2015).

Considerable interest is also attracted to icebergs of smaller sizes, below several nautical miles. Drifting patterns of small icebergs may be different from those of giant icebergs (e.g., Rackow and others, 2013). Despite being smaller these icebergs still can contribute significantly to the freshwater balance (Tournadre and others, 2016), affect ocean waves (Ardhuin and others, 2011) and interfere with ship navigation. In contrast to giant icebergs, information on smaller Antarctic icebergs with a size below several nautical miles down to 10–15 m is not collected systematically and a proper monitoring system has not been established.

In situ observations from ships have been traditionally used in studies of smaller icebergs (e.g., Wadhams, 1988; Orheim, 1990; Jacka and Giles, 2007). These observations are relatively sparse, unevenly cover the Southern Ocean and are often hard to compare and combine due to different observation protocols they follow. High spatial resolution remote-sensing data, in particular data from satellite-based

synthetic aperture radars (SAR) and satellite altimeters, present a potentially useful source of information on smaller icebergs (Williams and others, 1999; Wesche and Dierking, 2015; Tournadre and others, 2016). These techniques however are affected by a number of physical limitations, which hamper consistent and accurate iceberg retrievals over large areas. Sparseness of in situ observations of icebergs and weaknesses of available iceberg remote-sensing techniques cause a considerable uncertainty in the estimates of the small-iceberg concentration and its variability across the Southern Ocean. This also concerns estimates of the total number of smaller icebergs and their surface area, weight and volume.

In the past decade, joint efforts between Shirshov Institute of Oceanology of Russian Academy of Sciences and Arctic and Antarctic Research Institute (AARI) have been undertaken to improve characterization of Antarctic icebergs using in situ ship observations. Within this program iceberg observational data were recovered from historical ship log journals archived at AARI, obtained from published reports and acquired from various internet resources. As a result, we have compiled one of the largest datasets of in situ iceberg observations. The dataset currently incorporates more than 60 000 records collected since the late 1940s characterizing the iceberg concentration, size distribution and iceberg shapes. Using this dataset we produced a detailed map of the iceberg distribution in the Atlantic and Indian sector of the Southern Ocean (Romanov and others, 2008), characterized the seasonal change of iceberg concentration (Romanov and Korotkov, 2001), compiled and summarized the available statistics on the iceberg frequency distribution by shape and size (Romanov and others, 2012) and characterized the iceberg response to El Niño and El Niño Modoki (Romanov and others, 2014).

In recent years the iceberg dataset has been complemented with both recovered historical data and observations obtained in recent (2007–14) cruises of AARI ships in Antarctica. The updates comprising more than 10 000 iceberg observation records of various types increased the total volume of the dataset by more than 20%. In this study, we analyze this updated dataset to establish a more accurate and spatially detailed characterization of the iceberg distribution over the entire Antarctic region. The objective of the work was also to complement estimates of the mean iceberg concentration across the Southern Ocean with more detailed statistics including the iceberg concentration minimum and maximum values and variability. The focus of the study has been on small and medium-size icebergs with sizes below several nautical miles.

In this paper, we first give an overview of iceberg observation techniques and datasets. The review is followed by a description of the collected ship-based iceberg observation dataset and the technique we have used to establish the iceberg distribution over the Southern Ocean. The iceberg distribution is examined and explained with respect to the atmospheric circulation and ocean currents. Information on the iceberg concentration along with information on the iceberg morphometric characteristics, in particular, their shape and size, is further used to estimate area-integrated characteristics of Antarctic icebergs including their total number, area extent, and volume.

Throughout the paper the term ‘mean’ is used to define iceberg characteristics averaged over the 60+ year period

covered by the dataset. The term ‘total’ represents area-integrated instantaneous characteristics of the icebergs (total number, area and volume) in the entire Antarctic region.

ANTARCTIC ICEBERG OBSERVATIONS: TECHNIQUES AND RESULTS

Available information on the distribution of small and medium-sized icebergs in the Southern Ocean comes primarily from two major sources: satellite-data-based estimates and in situ ship-based observations. Both approaches and corresponding datasets have their own advantages and weaknesses.

The high spatial resolution and all-weather capability of satellite-based SAR make these observations attractive for monitoring Antarctic icebergs. Examples of applications of SAR data to estimate the iceberg concentration and iceberg drift patterns over the Weddell Sea and over the Indian Ocean Sector of Antarctica have been presented correspondingly by Gladstone and Bigg (2002) and Young and others (1998). Wesche and Dierking (2015) identified icebergs in the SAR-based mosaic over Antarctica and found considerable regional variations in the iceberg size distribution. Speckles affecting SAR imagery present a serious issue complicating both automated and manual identification of small icebergs with a size of less than several SAR pixels (or below ~100 m). Until the recently rare availability of the imagery over the Southern Ocean and its high-cost limited iceberg monitoring with SAR data. This situation is expected to improve with the recent launch of Sentinel-1 satellites providing free high spatial resolution radar imagery to the public.

Satellite altimeter data present another source of information on Antarctic icebergs. Retrieval technique and first results of iceberg identification with altimeter data are presented by Tournadre and others (2008, 2012). A more comprehensive processing of altimeter observations since 1994 resulted in an extensive iceberg dataset and a corresponding spatially-detailed map of iceberg concentration in the Southern Ocean (Tournadre and others, 2016). Similar to SAR, radar altimeter observations are weather independent; however, iceberg identification with altimeter data requires ice-free water conditions and relies on the assumed iceberg freeboard elevation and reflectivity. Furthermore, due to specifics of radar altimeter data retrievals are limited to icebergs with a height of <15 m and with a size between 0.3 and 8.0 km².

Ship observations, providing information on the concentration and the size of icebergs, have been used to characterize the Antarctic iceberg distribution since the early 1960s. Nazarov (1962) compiled a map summarizing Antarctic iceberg sightings since the late 18th century to the middle of the 20th century. According to this chart, icebergs were seen as far north as 40° S in the Atlantic and Indian sectors and up to 50° S in the Pacific sector of the Southern Ocean. One of the first charts of iceberg drift in Antarctica was presented by Shilnikov (1969). Buinitskii (1973) produced a map of the mean iceberg concentration in the Indian Ocean sector of the Southern Ocean. Burrows (1976) compiled information on the largest distance from the coast of Antarctica where icebergs were sighted. According to his study icebergs can travel as far north as 30°–34° S within 90° W to 90° E longitudes and up to 40°–42° S within 90° E–90° W. Later studies however never confirmed iceberg sightings at such low latitudes (e.

g., Orheim, 1990). Gradual accumulation of in situ iceberg observation data in the last three decades has allowed for a progressively more detailed characterization of the spatial distribution of Antarctic icebergs in various regions of the Southern Ocean (Wadhams and others, 1988; Koshlyakov and others, 1993; Romanov, 1996a, b; Jacka and Giles, 2007; Romanov and others, 2008; Orheim, 2015) as well as their seasonal changes (e.g., Romanov and Korotkov, 2001; Romanov and Romanova, 2003, 2005).

There is a substantial interest in estimating area-integrated characteristics of icebergs, particularly their number, surface area and volume. This information presents an important input to studies and estimates of the iceberg calving rates, freshwater flux provided by icebergs, global sea-level change, mass balance of the Antarctic ice sheet and the iceberg impact on the Antarctic ecosystem dynamics. Silva and others (2006) used satellite-based information on the size of giant icebergs calving off Antarctic ice shelves and found that the mass of these icebergs can reach $\sim 6000 \text{ Gt a}^{-1}$. The annual mass of calving icebergs averaged over the time period from 1979 to 2003 however was noticeably smaller and amounted to $1089 \pm 300 \text{ Gt}$. Given an assumed ice density of 850 kg m^{-3} (Jacobs and others, 1992) this equates to a freshwater volume of $1281 \pm 353 \text{ km}^3$. Considerably larger estimates of the total iceberg volume, of $22\,000 \text{ km}^3$ in 2002 and 9000 km^3 in 2012, are given by Tournadre and others (2015), who used NIC and Brigham Young University data on large icebergs. Wesche and Dierking (2015) placed the estimated instantaneous mass of Antarctic icebergs to within $5167\text{--}7440 \text{ Gt}$ (or $6079\text{--}8753 \text{ km}^3$); however, this estimate included only icebergs in the near coastal zone. Tournadre and others (2012) examined smaller icebergs with a size of $100\text{--}2800 \text{ m}$ in the area north of 66° S and estimated their weight equal to 400 Gt . Expanding the analysis to Antarctic coastal waters these authors obtained an estimated total weight of icebergs of $\sim 600 \text{ Gt}$, which is equivalent to the volume of 706 km^3 (Tournadre and others, 2016).

Similar to the satellite-based remote-sensing retrievals, estimates of the total mass and volume of Antarctic icebergs derived from ship observations also vary substantially. The range of reported estimates of the total volume of icebergs simultaneously floating or grounded in the Southern Ocean (or instantaneous iceberg volume) spans from 4700 km^3 (Romanov, 1996a) to $17\,900 \text{ km}^3$ (Shilnikov, 1960). Other estimates of the total iceberg volume amounting to 5600 , 8200 , $12\,000$ and $12\,500 \text{ km}^3$ have been provided correspondingly by Buinitskii (1973), Schell (1974), Losev (1982) and Orheim (1985).

A wide spread in the estimated values of the iceberg volume is due to high spatio-temporal variations of the Antarctic icebergs distribution and to a relatively small number of available iceberg observations. Most estimates of the total iceberg count and iceberg volume in Antarctica have been made using observations over a limited area and extrapolating the results to the entire Southern Ocean (e.g., Buinitskii (1973), Shilnikov (1960), Losev (1982)). Another reason for the large scatter in the estimated total volume of icebergs is uncertainty with respect to geometrical characteristics of icebergs, particularly to their size and shape. Assumptions on the iceberg geometrical properties, particularly on the relationship between the iceberg length, width and height and on their shape varied from one study to another and often were based on very limited statistics.

Generating more accurate and more physically justified estimates of the iceberg volume and mass requires utilizing more spatially extensive and detailed information on the iceberg concentration and improved statistics of the iceberg morphometric properties.

IN SITU ICEBERG OBSERVATIONS DATASET

The Antarctic iceberg dataset collected and maintained jointly by Shirshov Institute of Oceanology of the Russian Academy of Sciences and AARI incorporates information obtained through iceberg observations from ships traveling in the Southern Ocean. The dataset is routinely updated with recent observations and newly recovered historical data. The core of the dataset comprises $\sim 45\,000$ iceberg observation reports delivered since the middle of the 1950s from the research vessels of AARI. These data were rescued and recovered from the original ship ice and weather log journals archived at AARI. Most reports provide only the number count of icebergs sighted by the observer. The dataset also incorporates the results of ~ 4000 ship observations of icebergs performed according to the guidelines of the Norwegian Polar Institute, NPI (Orheim, 1980) over the period from 1978 to 1987. Within this program observers were requested to report the iceberg amount within five size range categories, $10\text{--}50$, $50\text{--}200$, $200\text{--}500$, $500\text{--}1000$ and 1000 m . The results of ~ 7000 observations conducted under the auspices of the Australian Antarctic Program (AAP) during the period from 1978 to 2001, were acquired from the dataset compiled by Dr T. Jacka (https://data.aad.gov.au/metadata/records/climate_iceberg). Similarly to NPI, AAP iceberg reports included both the total number of icebergs and the iceberg quantity in a number of size categories. The AAP size categories however were different from those of NPI and covered a wider range from 25 to 3200 m . Finally, over 4000 iceberg records made in Antarctica from Russian whaling ships in $1947\text{--}59$ were recovered from various reports on these cruises. The majority of observations incorporated in the dataset ($\sim 90\%$) were performed during the warm season from December to April (see Table 1).

In about three-quarters of observation records comprising the dataset, icebergs have been identified and counted using the ship radar. The remainder of reports, mostly dating back to the $1940\text{--}1960\text{s}$, are based on visual observations. In the reports, information on the iceberg concentration is provided as the number count of icebergs within a circle of a certain radius. Both the size of the circle and the time interval between consecutive observations may vary. At AARI the radius of the circle is set to 15 nm (27.8 km), whereas observations are typically performed every $1.5\text{--}3 \text{ h}$. The time interval varies depending on the ship speed to avoid overlapping of the observing circles and double-counting of the icebergs. When examining and processing the data we did not specifically check for possible multiple recording of the same icebergs by two or more ships traveling in the same region at the same time since these instances are very rare.

The NPI guidelines instruct to report the number of icebergs within a circle of 12 nm radius and to perform observations every 6 h . Within the AAP iceberg counts were performed every 3 h within a smaller, 6 nm range. In both latter cases, the ship velocity of 4 knots or higher ensures no overlap of consecutive observations. Within all three major iceberg observation programs (NPI, AAP and AARI) observers report cases when no icebergs were seen. These

Table 1. Distribution of observation records of the iceberg concentration by the month of the year

Month	Jan	Feb	Mar	Apr	May	Jun	Jul	Aug	Sep	Oct	Nov	Dec	Total
Number of Observation Records	12 464	11 759	11 815	5845	2362	702	482	155	226	1103	2099	9825	58 837

observations are recorded as 'no iceberg sightings', to distinguish between cases where there were no icebergs and where no observations were made.

Routine iceberg observation and reporting typically starts with the sighting of the first iceberg on the ship route and ends when on several consecutive observation times no icebergs were observed. The lack of explicit 'zero' iceberg number reporting immediately north of the location of the first and of the last iceberg sighted presents a considerable problem since it causes an overestimate of the mean concentration in the area of intermittent iceberg occurrence. To ensure adequate characterization of the iceberg distribution across the Antarctic region, in this study the AARI iceberg records were complemented with synthesized 'no iceberg sighting' reports. These reports were generated for the time and location of each meteorological observation taken at 3 h time interval along the ship route south of 46° S preceding the first and following the last iceberg sighting.

When processing the iceberg observation data we consider iceberg counts obtained from visual and from radar observations comparable. This approach is justified by the results of Dowdeswell and others (1992) who reported only a small, within 5%, the difference between the iceberg amounts estimated visually and with the radar-based technique. Reported iceberg quantities are also corrected to account for a gradually decreasing success rate of radar-based iceberg detection with distance from the radar. Following Wadhams (1988) we assume a linear decrease of the detection success rate from 100% at 8 nm to 0% at 22 nm. To achieve consistency between observations made over different areas we adopted the 15 nm range as a standard and adjusted all reported iceberg quantities to this range. For convenience in this paper, the iceberg quantity within the standard 15 nm distance range is further referred to as the iceberg concentration. Simple geometrical considerations allow for converting this value to the number of icebergs within a certain area, e.g., the iceberg concentration of 100 corresponds to approximately four icebergs per 10 km × 10 km square box.

Aside from the iceberg number counts more detailed iceberg observations that specifically focused on the iceberg shape characterization were conducted during several cruises of *r/v 'Professor Wiese'* in 1973–90. During these cruises the iceberg concentration observations were complemented with counts of the number of icebergs of different shapes. The reports included both the overall amount of iceberg sighted and the number count of icebergs of each of five basic shapes, tabular, dome-shaped, sloping, pinnacle

and weathered. The dataset includes 1777 such 'iceberg number count by shape' observations incorporating information on more than 21 000 individual icebergs.

In a number of AARI cruises, observations of the iceberg concentration were accompanied by measurements of the morphometric characteristics of selected individual icebergs. The iceberg shape was determined visually whereas the iceberg length and freeboard elevation were measured with a sextant and a rangefinder. Our dataset contains information on geometrical parameters of 4130 icebergs of different shapes collected since 1957. Table 2 presents the distribution of the number of iceberg observations of the two latter types (iceberg number count by shape and iceberg geometry by shape) by the month of the year. Similar to the iceberg concentration, most these observations were performed during the warm season of the year.

Figure 1 shows the geographic distribution of collected iceberg number count records including synthesized zero iceberg concentration reports. This distribution is highly uneven: no records are available in the south-west of the Weddell Sea, in the southeast of the Pacific sector and in a number of coastal regions of the Indian Ocean sector of the Southern Ocean. At the same time, there is a large density in the coastal area within 60° E to 120° E next to the location of most Russian and Australian Antarctic stations and within 60° W to 50° E longitude away from the coast. These areas are most frequently traveled through by Antarctic supply ships. Similar to the iceberg concentration measurements, most detailed observations of the iceberg shapes and geometrical characteristics have been conducted in the Atlantic sector of the Southern Ocean (see Fig. 2).

ICEBERG CONCENTRATION AND GEOGRAPHICAL DISTRIBUTION

Figure 3a presents a map of the mean iceberg concentration in the Southern Ocean derived from the iceberg concentration reports contained in the collected dataset. The map was generated by aggregating all available iceberg observation records within 1° latitude and 2° longitude grid cells, bringing the reported iceberg number count to the standard 15 nm range and averaging this number within each grid cell. As such the map is meant to represent the average (or the most typical instantaneous) distribution of the iceberg concentration in the Southern Ocean over the 60+ years period covered by the dataset.

The map in Fig. 3a distinctly shows three known clusters of elevated iceberg concentration in Antarctica located in

Table 2. Number of available detailed observations of iceberg shape and size by the month of the year

Month	Jan	Feb	Mar	Apr	May	Jun	Jul	Aug	Sep	Oct	Nov	Dec	Total
Iceberg number count by shape	527	223	485	19	–	–	–	–	–	–	–	523	1777
Iceberg geometry by shape	1349	739	674	365	50	5	–	–	34	40	61	813	4130

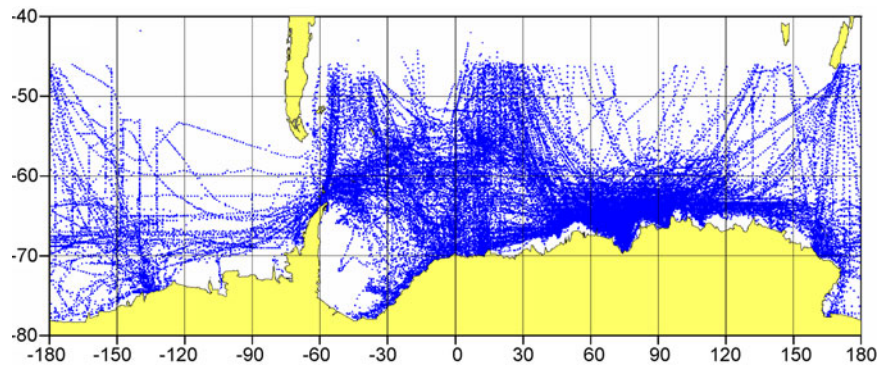


Fig. 1. Location of ship observations of the iceberg concentration in the Southern Ocean performed during the time period from 1958 to 2014. Eastern longitudes are positive and western longitudes are negative.

the Atlantic Ocean within 0° – 60° W, in the Indian Ocean within 40° – 120° E and in the Southern Pacific within 90° – 170° W (e.g., Schodlok and others, 2006, Jacka and Giles, 2007, Romanov and others, 2008, Orheim, 2015, Tournadre and others, 2016). The area in the Atlantic Ocean corresponding to the Weddell Sea has the maximum northward extension with large numbers of icebergs north of 50° S. At the same time the largest iceberg concentrations, often exceeding 30 icebergs within a 15 nm range, occur in the other two areas in the Indian and Pacific Sectors of the Southern Ocean.

In the coastal zone, the iceberg concentration depends on the productivity of nearby glaciers, their structure (Rignot and others, 2013; Wesche and others, 2013), the prevailing ocean currents and peculiarities of the bottom topography. In particular smaller iceberg concentrations are observed at 20° – 35° E next to the Princess Ragnhild Coast where there are no productive glaciers (Williams and Ferrigno, 1988; Rignot and others, 2013). Iceberg drifting to this region with the coastal eastward-ward current is hampered by a sharp cape at $\sim 34^{\circ}$ E and the area of shallow waters extending northwards of this cape. Larger iceberg concentrations are seen at the location of Amery ($\sim 70^{\circ}$ E– 75° E), Shackleton ($\sim 95^{\circ}$ E– 100° E), West (80° E– 90° E) and Getz ($\sim 120^{\circ}$ W– 140° W) ice shelves.

Away from the shore the spatial distribution of the iceberg concentration is determined to a large extent by peculiarities of the atmospheric circulation. In summer, from October to March, three stable cyclonic pressure systems develop in the Southern Ocean with centers at $\sim 120^{\circ}$ W, 30° E and 110° E (see Fig. 3b). Southerly winds at the western periphery of these pressure systems transfer a large number of icebergs to the north into the open ocean and thus cause the increase of their concentration. Northerly winds at the eastern periphery of atmospheric cyclones cause icebergs to drift closer to

the coast creating large areas of small iceberg concentrations in the open ocean to the east, and sometimes in the center of these cyclones. The stability of the pattern of the atmospheric circulation throughout the year ensures the stability of this iceberg distribution pattern.

An interesting feature in the iceberg distribution is their relatively small concentration in the Ross Sea region (160° E to 150° W) both along the coast and further out in the open ocean, which may seem inconsistent with the presence of the large Ross Ice Shelf. A feasible physical explanation of small concentrations of icebergs in the Ross Sea is that southerly winds prevailing in this region (Nigro and Cossano, 2014) may be sufficiently stable and strong to ensure a rapid removal of icebergs along with the sea ice away from the coast. An overall small number of icebergs may also be due to the fact that the Ross Ice Shelf tends to generate predominantly large icebergs. Support for this latter hypothesis is provided in particular by Wesche and others (2013) who observed a specific structure of cracks in the Ross Ice Shelf.

The eastern periphery of one of the low-pressure regions in Antarctica is steadily located over the west of the Weddell Sea, west of 40° – 50° W (see Fig. 3). Therefore winds of northerly directions should dominate here throughout the whole year. These winds are generally expected to prevent the removal of icebergs from this region to the north and northeast. The fact that a large number of icebergs is observed in the northwestern Weddell Sea, west of 30° W, indicates that iceberg drift patterns in the Weddell Sea are mostly determined by ocean currents.

As seen in Fig. 3, the northern boundary of the iceberg occurrence (NBIO) essentially coincides with the position of the oceanic Polar Front (PF). This can be explained by a so-called zone of oceanic convergence associated with the PF, where southerly and northerly flows at the ocean

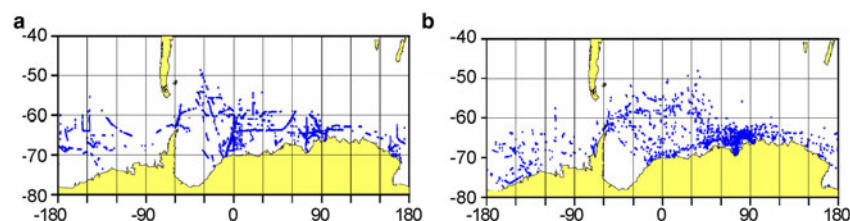


Fig. 2. Location of detailed observations of iceberg properties. (a) Observations of number count by shape made from the *r/v* 'Professor Wiese' in 1980–1988. (b) Observations of iceberg geometry by shape made in 1957–2014. Eastern longitudes are positive and western longitudes are negative.

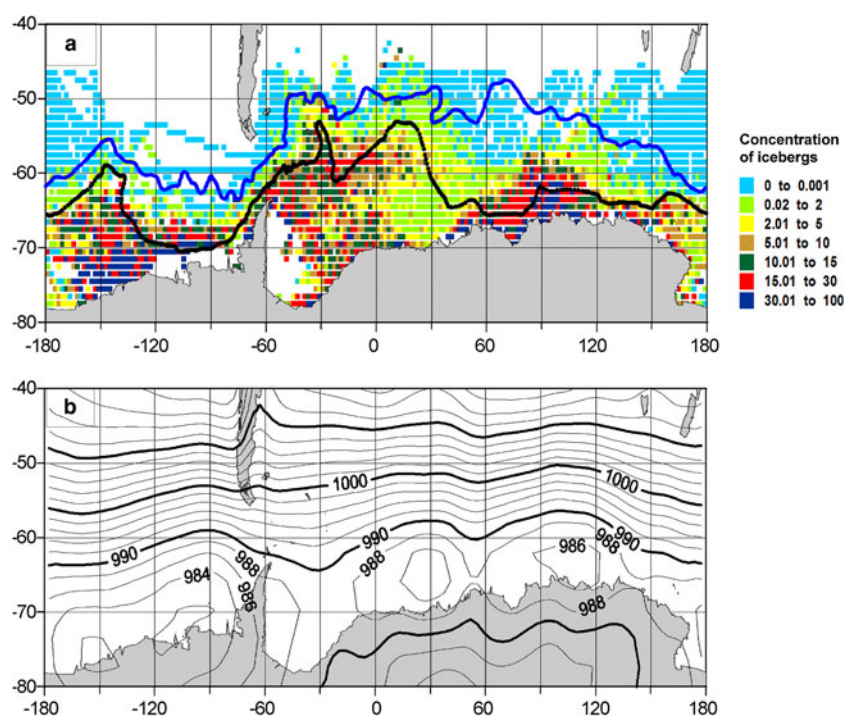


Fig. 3. (a) Map of the mean iceberg concentration in grid cells of 1° latitude by 2° longitude. Iceberg concentration is expressed as the number of icebergs sighted within 15 nm range from the ship). Grid cells with no observations are left blank. The blue line shows the location of the polar ocean front; the black line shows the southern boundary of the ACC according to Orsi and Ryan (2001). (b) Mean atmospheric pressure at sea level (hPa) from October to March over the 60-year period from 1950 to 2010 calculated using monthly mean sea surface pressure data of Hadley Centre (<http://hadobs.metoffice.com/hadslp2/data>).

surface converge and thus prevent icebergs from drifting into lower latitudes. The PF is also associated with a large temperature contrast of sea-surface waters. When examining temperatures in the 0–200 m top ocean layer in the Drake Passage, Sprintall and others (2012) found a substantial temperature change from 3 to 5 °C north of the PF down to –1 °C immediately to the south. It is obvious that icebergs would be more sustainable in colder waters south of the PF than in warmer waters north of it.

In some areas, however, the NBIO clearly deviates from the PF. This happens in particular, at 50°–80° E where it is located considerably south of the PF. We attribute this to the fact that at these longitudes there is no iceberg removal from coastal areas to the north whereas icebergs carried out of the Weddell Sea and drifting eastward along with the Antarctic Circumpolar Current (ACC) decay before reaching these longitudes. An opposite situation is seen at 0°–30° E longitude where NBIO extends northwards past the PF and reaches 44°–46° S parallel. Penetration of icebergs to such low latitudes may be facilitated by frequent oceanic eddies that develop at the borders of the ACC and Agulhas current (e.g., Dencausse and others, 1989). Another region where Antarctic icebergs are frequently seen beyond the PF is located at ~100°–120° E. The band of larger iceberg concentration extending north-east past 50° S and crossing the PF in this region is created by a strong northward ocean current component at ~85° E, east of Kerguelen Plateau (McCartney and Donohue, 2007). It causes icebergs to escape from the coastal current and drift northward. Some of these icebergs occasionally reach the coast of New Zealand (Burrow, 2005).

Although the number of available iceberg reports is relatively large, they are distributed across the Antarctic region unevenly leaving some areas of Antarctica with no records at all. As seen in Fig. 4a, the coverage of the Atlantic and

Indian sector of the Southern Ocean with iceberg observation data is clearly better than the coverage of the Pacific sector. Variability of the iceberg occurrence (Fig. 4b) exhibits a spatial pattern similar to the one seen in the distribution of the mean values. The RMS deviation of the iceberg concentration averaged over all ocean grid cells covered with observations amounted to 8.0, which is almost equal to the grid cell mean value of the iceberg concentration of 8.4. Further analysis of the iceberg observation statistics shows that cases with no icebergs in sight occur quite often. Non-zero minimum iceberg concentration is found only in ~15% of all grid cells. Figure 4c shows that in the Eastern Hemisphere these grid cells are located mostly within a narrow coastal zone whereas in the Western Hemisphere such locations are found both in the coastal area and in the open ocean. The spatial distribution of the maximum iceberg concentration (Fig. 4d), iceberg-free occurrence (Fig. 4e) and the frequency of occurrence of iceberg concentration of over 10 icebergs per circle of 15 nm radius (Fig. 4f) generally follows the spatial distribution of the mean iceberg concentration. The maximum iceberg concentration along with the smallest values of the iceberg-free occurrence corresponds to the Weddell Sea and the area north of it within 0°–60° W, the coastal zone next to Amery, West and Shackleton glaciers, within 60°–120° E, and to the Ross and Amundsen Sea region within 120°–160° W.

The amount of available iceberg observations presents a factor affecting the derived statistics of the iceberg concentration. This concerns primarily the minimum and maximum values of the iceberg concentration, which tends correspondingly to decrease and increase with increasing size of the sample. Therefore estimates of extreme values of the iceberg concentration made for grid cells with few observations may not be reliable and should be used with care.

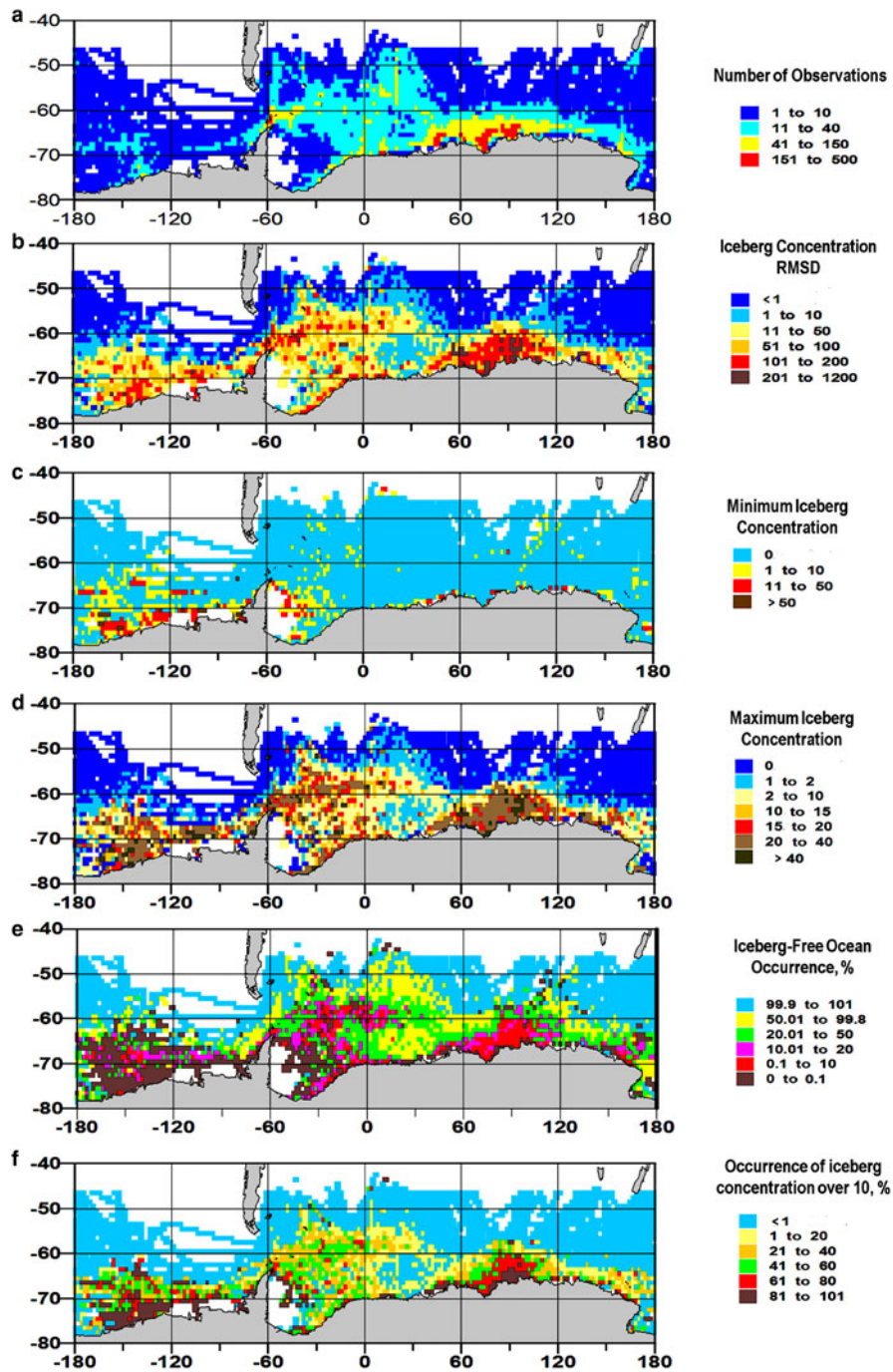


Fig. 4. Iceberg statistics. (a) The number of iceberg number count reports in grid cells of 1° latitude by 2° longitude. (b) Standard deviation of the observed iceberg concentration. (c) Minimum observed iceberg concentration. (d) Maximum observed iceberg concentration. (e) Frequency of occurrence of iceberg-free waters (in percent). (f) Frequency of occurrence of the iceberg concentration exceeding ten icebergs within the circle of 15 nm radius (in percent) Iceberg concentration is expressed as the number of within a circle of 15 nm radius.

This applies in particular to the Pacific sector of the Southern Ocean and to the central part of the Weddell Sea where most grid cells are covered with fewer than ten reports of the iceberg concentration. Estimates of the mean iceberg concentration may also be affected by the limited number of observations. As was shown earlier there is good correspondence between the derived iceberg concentration and major physical factors controlling the iceberg distribution (i.e. glacier productivity, wind and ocean current patterns). This may be considered as evidence that despite a small number of observations in some areas the derived map of the iceberg concentration realistically characterizes the iceberg distribution in Antarctica.

TOTAL ICEBERG COUNT

An estimate of the total instantaneous number of icebergs in Antarctica has been obtained through integration of the derived spatial distribution of the iceberg concentration over the surface of the Southern Ocean. Discontinuities in the iceberg concentration map caused by unavailability of iceberg observations were eliminated with two different techniques. A simple bilinear interpolation has been applied to fill in gaps in the area coverage of the available iceberg concentration map in the open ocean. In the coastal areas, characterized by potentially large spatial gradients of the iceberg concentration, we have used a more sophisticated approach,

which accounts for the proximity of iceberg-generating glaciers and their productivity.

In this latter approach, the relationship between the glacier characteristics and the iceberg concentration in adjacent coastal zones was established using estimates by Rignot and others (2013) of the Antarctic glaciers ice front flux, which is the proxy for the calving flux or glacier productivity. These data were matched with the mean iceberg concentration calculated for grid cells of 2° latitude by 5° longitude adjacent to the glacier location. Only grid cells with over 30 iceberg observation records were used. From more than 60 glaciers surveyed by Rignot and others (2013) sufficient matching iceberg concentration data were found for 23 glaciers. A certain weakness of this approach consists in the fact that information on the glacier productivity rates and iceberg concentration does not quite match in time: Rignot and others (2013) estimates generally represent the calving flux in the first decade of the 21st century whereas collected iceberg concentration data refer to the last 60+ years time period. Still the correlation statistics presented in Table 3 and a corresponding plot in Fig. 5 demonstrate a well-pronounced positive correlation between the iceberg concentration and the glacier productivity ($R = 0.49$, $R^2 = 0.26$, statistically significant at the 0.01 level). The relationship between the two parameters was approximated with a

Table 3. Antarctic glaciers ice front flux (proxy for calving or productivity) in Gt a^{-1} according to Rignot and others (2013), mean iceberg concentration (expressed as the number of icebergs within a circle of 15 nm radius) and the number of iceberg observation reports within grid cells of 2° latitude by 5° longitude adjacent to the glacier. Productivity estimates for closely located glaciers are combined

Glacier	Glacier productivity, Gt a^{-1}	Mean iceberg concentration	Number of observations
Drigalski	3.2	6.3	33
Nansen			
Aviator	0.8	3.8	72
Mariner			
Lillie Rennick	1.3	24.6	304
Mertz	12.0	11.4	222
Dibble	8.2	13.2	125
Totten	28.0	16.9	229
Vincennes	6.8	21.7	421
Shackleton	30.3	45.2	230
West	32.6	30.9	697
Publication	55.6	50.4	1034
Amery			
Baudouin	6.5	1.4	58
Borchgevink	17.5	5.5	225
Lazarev Nivl	4.4	43.2	636
Vigrid	2.0	7.8	158
Fimbul Jelbatrt	27.0	26.4	116
Atka, Quar	3.9	26.1	97
Ekstrom			
Riiser-Larsen	12.1	23.7	103
Brunt/	28.1	23.0	39
Stantomb			
Filchner	82.8	22.7	114
Cosgrove Pine Island	63.6	90.0	34
Getz	53.5	37.4	38
Land	12.2	36.1	37
Nickerson	4.3	47.7	53

linear function ($Y = 0.45X + 17.00$) and was further applied to estimate the iceberg concentration in the coastal grid cells adjacent to glaciers where in situ iceberg observations were lacking.

Figure 6a presents a map of the iceberg concentration where all discontinuities in the area coverage were removed either through interpolation or by filling in values predicted from the glacier productivity data. The map has been produced on a coarser resolution grid with 2° latitude and 5° longitude grid cell size. Grid cells where the interpolation procedure was applied are shown in Fig. 6b. The total number of icebergs in the Southern Ocean was then estimated by converting the estimated mean iceberg number count within 15 nm range to the iceberg quantity per unit area in individual grid cells and aggregating the results over all ocean grid cells. In the coastal areas the total number of icebergs in the grid cell was adjusted with respect to the actual area fraction of the ocean surface in the grid cell.

The estimated number of icebergs in the entire Southern Ocean amounted to 132 269. This value is larger than 100 000 given by Romanov (1996a, b) but noticeably smaller than the estimate of Orheim (1980) who put it to 200 000–300 000. The uncertainty in the estimated total number of icebergs was calculated using information on the variability of the iceberg concentration in individual map grid cells and amounted to ± 9341 or $\sim 7\%$ of the magnitude. Estimates of the total iceberg amount within different latitude bands and different sectors of the Southern Ocean are shown in Table S1 in the Supplementary Materials section. The majority of icebergs are found in the Pacific Ocean, somewhat fewer icebergs in the Atlantic and even fewer in the Indian Ocean sector. The latter is not surprising, given that the coast of Antarctica passes much farther north in the Indian Ocean Sector than in other sectors of the Southern Ocean.

TOTAL AREA AND VOLUME OF ANTARCTIC ICEBERGS

Estimating other area-integrated characteristics of Antarctic icebergs, namely their total area and volume, requires information on the iceberg geometrical characteristics, length, width, height, shape and their distribution across the Southern Ocean. Available direct measurements of the iceberg geometrical parameters are sparse and are hardly sufficient to adequately characterize the iceberg sizes

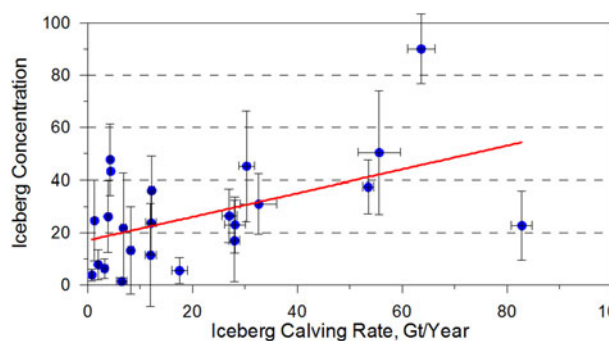


Fig. 5. The relationship between the productivity of 23 Antarctic glaciers (see Table 3), and the iceberg concentration in grid cells adjacent to the glacier location. Iceberg concentration is expressed as the number of icebergs within a circle with a radius of 15 mm. Linear regression equation (red line in the graph) is $Y = 0.45X + 17.00$, $R = 0.49$, $R^2 = 0.26$.

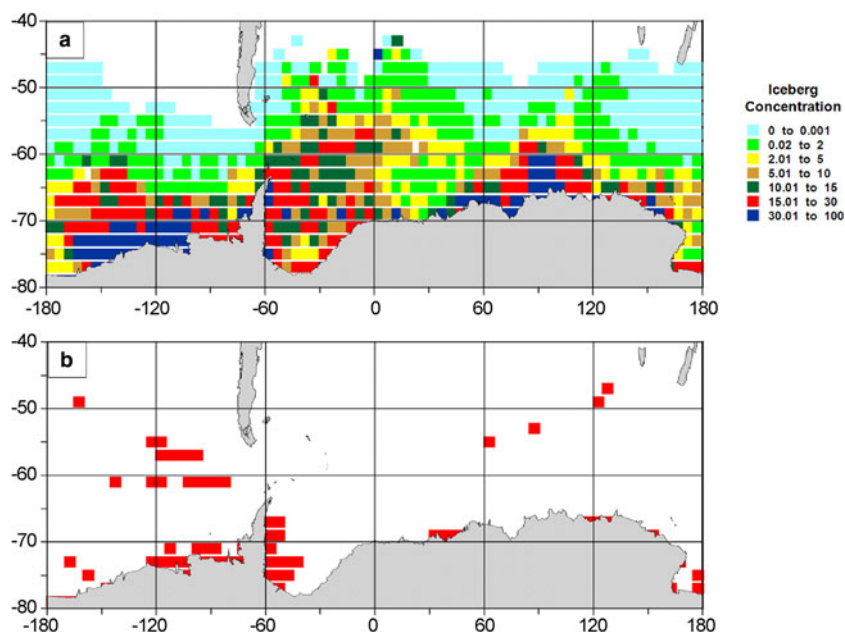


Fig. 6. (a) Estimated iceberg concentration in grid cells of 2° latitude by 5° longitude. (b) The location of grid cells where gaps in the observation-based iceberg concentration map were filled in through interpolation, or using the relationship between the iceberg concentration and the glacier productivity. Iceberg concentration is expressed as the number of icebergs within a circle with a radius of 15 mm.

everywhere in Antarctica. Therefore in this study, we implemented a different approach where estimates of the iceberg area and volume were derived from spatially-distributed estimates of the iceberg concentration (presented earlier in the paper), statistics of the iceberg occurrence by shape and information on geometrical parameters of icebergs of different shapes.

The cumulative area of all icebergs within each grid cell was estimated as the sum of mean areas of icebergs of five major shapes (table, dome, pinnacle, sloping and weathered) weighted by the fraction of icebergs of each shape and multiplied by the number of icebergs of all shapes in the grid cell. The same algorithm but with the mean iceberg area extent replaced by the mean volume was applied to estimate the total ice volume in icebergs within a grid cell. The total area (A) and the total volume of icebergs (V) in the Southern Ocean were then calculated by summing correspondingly estimates of the area and the volume of icebergs in individual grid cells:

$$A = \sum_i \sum_j C_i F_{ij} A_{ij}$$

$$V = \sum_i \sum_j C_i F_{ij} V_{ij}$$

where C_i is the number of icebergs in grid cell i , F_{ij} is the mean fraction of icebergs of shape j in grid cell i , A_{ij} and V_{ij} are the mean area extent and the mean volume of icebergs of shape j in grid cell i . Summing is performed across all grid cells (i) and all five iceberg shapes ($j = 1 \dots 5$).

To calculate the iceberg area and volume within each grid cell we have used estimates of the percent fraction of icebergs of each type and information on the mean size of icebergs of different shapes in the Southern Ocean provided in Romanov and others (2012). These location-dependent estimates were derived from ~3000 AARI ship observations

made in 1957–2009. In the current study, the statistics of geometrical characteristics of the iceberg of different shapes was complemented by over 1000 observation records made in the last 5 years, from 2009 to 2014. The updated statistics of the frequency of occurrence of icebergs of various shapes in the Southern Ocean along with estimates of the mean freeboard height, length, area and volume of Antarctic icebergs of different shapes are presented correspondingly in Tables S2 and S3 in the Supplemental Materials section. Even with the added data, the available statistical information on the iceberg shape and size was insufficient to reliably characterize these parameters within each individual grid cell. Therefore spatial averaging of the data has been applied. To establish the percent fraction of icebergs of each shape (F_{ij}) all reported iceberg number distributions by shape were aggregated and averaged within 4° latitude intervals in the Western and in the Eastern Hemisphere (see Supplementary Table S2). Data on the length and the freeboard of individual icebergs of different shapes contained in the iceberg geometry dataset were aggregated and averaged within two latitude zones, north and south of 66° S (Supplementary Table S3).

The area of each individual iceberg in the iceberg geometry dataset was calculated as the product of its length and width multiplied by a corrective factor accounting for a non-rectangular shape of the iceberg. The width of the iceberg was estimated from its length using a length to width ration of 1.56 proposed by Dmitrash (1973) and Shilnikov (1960). A similar ratio of 1.50–1.62 were reported by Bigg and others (1997) and Dowdeswell and others (1992), whereas somewhat smaller values of 1.35–1.47 were given by Young and others (1998). The value of the corrective factor accounting for a non-rectangular shape of the iceberg was set equal to 0.755, which is the mean of the corresponding estimates of Dmitrash (1973) of 0.91 and Shilnikov (1960) of 0.6. The corrective factor value of 0.755 we adopted in this study is close to 0.785 proposed

by Jacobs and others (1992). The latter value corresponds to the ratio of the area to the product of the length and the width of an ellipse.

The volume of each iceberg was calculated as the product of the iceberg area and thickness. The iceberg thickness was determined from its freeboard following Shilnikov (1969) who found the freeboard to thickness ratio of 1:7 for tabular, domed and pinnacle icebergs and 1:4 for sloping and weathered icebergs. This approach applied to all icebergs in our iceberg geometry dataset yielded the iceberg mean thickness of 292 m. The latter value is close to 250 m established for Antarctic icebergs by Jacobs and others (1992).

Using the approach described above we estimate of the instantaneous total area of Antarctic icebergs (with sizes <10 nm) equal to 57 805 km² (see Table 4). This corresponds to the area of one square iceberg with the length of ~240 km and is 6.5 times larger than the area of the largest iceberg B-15 calved from the Ross Ice Shelf in 2000 (Fricker and others, 2002). The uncertainty associated with the estimated total area of icebergs is determined by the uncertainty in the iceberg concentration within each map grid cell and the uncertainty of the mean area of icebergs of each shape. For the total area extent of icebergs in Antarctica the associated uncertainty was equal to ±18 410 km² or ~32% of the value. The total volume of all icebergs amounted to 16 893 km³ with an uncertainty of ±5609 km³ or ~33% of the value. Similar to the iceberg area, the uncertainty in the estimated iceberg volume results from the uncertainty in the iceberg concentration within each map grid cell and uncertainty in the volume of icebergs of each shape.

The largest amount of icebergs and therefore their largest area extent and volume are found in the Pacific sector of the Southern Ocean (see Table 4). There is a somewhat larger number of icebergs in the Atlantic sector than in the Indian Ocean (43 655 vs. 35 655); however owing to a more frequent occurrence of large tabular and dome-shaped icebergs, the area and the volume of icebergs in the Indian Ocean sector are slightly larger. It is important to note that although large tabular and dome icebergs represent only ~24% of all icebergs (23.3% in the Western Hemisphere sector and 24.9% in the Eastern Hemisphere sector), they contribute 95.1% to the area and 96.6% to the volume of all Antarctic icebergs. Decaying or weathered icebergs comprising ~65% of all icebergs in the Antarctic account for only 3.0% of the total iceberg area and 1.8% of the volume.

Our estimates of the total area extent and volume of Antarctic icebergs of 16 893 km³ is within the range of values reported in other iceberg studies but generally larger than the majority of these estimates. The latter concerns in particular Wesche and Dierking (2015) who reported the instantaneous total weight of Antarctic icebergs within 5167–7440 Gt (or 6079–8753 km³ iceberg volume) and Tournadre and others (2016) who estimated the total weight of small and medium-sized icebergs in the Southern Ocean equal to ~600 Gt (or ~706 km³). About two times smaller estimates of the iceberg volume by Wesche and Dierking (2015) as compared with our study may be explained by the fact that this research accounted for icebergs located only within 20–300 km off the coastal line. In Tournadre and others (2016) underestimation of the iceberg volume may have occurred due to the application of a satellite altimeter-based technique, which provides reliable iceberg identification only over ice-free water. Our estimate

of the total volume of icebergs also exceeds the estimate of Romanov (1996a, b) of 4700 and 12 000 km³ given by Orheim (1985) but is somewhat smaller than the total iceberg volume of 17 900 km³ reported by Shilnikov (1960). The two latter values, 17 900 km³ of Shilnikov (1960) and 12 000 km³ of Orheim (1985) fall within the uncertainty range of our estimate of the total iceberg volume.

Our estimate of the total volume of Antarctic icebergs of ~16.9 km³ (corresponding to the ice mass of ~15 000 Gt) may seem excessively large when compared with typical estimates of the yearly production of Antarctic glaciers ranging within 1000–2000 Gt a⁻¹ (e.g., Houghton and others, 1996; Silva and others, 2006; Depoorter and others, 2013). It is important however that the estimate of the iceberg volume is associated with large, ~30%, uncertainty. Similar if not larger uncertainty levels may be inherent in available productivity estimates (e.g., Silva and others, 2006). In particular, estimates of productivity of individual Antarctic glaciers and ice fields reported by Rignot and others (2013) and Gladstone and others (2001) differ in some cases by up to 5 times. Furthermore, the overall productivity varies substantially in time: it may reach 5000 Gt a⁻¹ in a case of a giant iceberg calving event (Silva and others, 2006). Lastly, there is a substantial uncertainty in the estimate of another component of the equation, the iceberg decay rate. Earlier estimates of the iceberg lifetime in the Southern Ocean ranged within 1–2 years (e.g., Orheim, 1980; Jacka and Giles, 2007); however recent studies show that it may be much larger, reaching 5–10 years (e.g., Rackow and others, 2017). Simple calculations show that for 2000 Gt a⁻¹ total iceberg productivity, 7 years iceberg lifetime and assumed exponential iceberg mass decay, the total mass of icebergs would noticeably exceed 13 000 Gt and therefore would agree within the quoted uncertainty level with our estimate of the total iceberg mass and volume.

Large, over 30%, uncertainties in the estimated values of the area and volume of Antarctic icebergs during the warm period of the year (December–April) may be attributed not only to relatively short-term spatial variability of the iceberg concentration and sizes caused mostly by processes of stochastic nature but partially to longer-term seasonal variations of the iceberg concentration. Shilnikov (1969) hypothesized that due to iceberg trapping in the sea ice the iceberg amount in the Southern Ocean should reach its maximum in September and October along with the extent of ice cover in Antarctica. As a result, a gradual decrease in the iceberg concentration should be expected in the course of the summer period. Evidence for the seasonal variability is provided in particular by Romanov and Korotkov (2001) who observed a more than the twofold reduction of the iceberg concentration in the open ocean part of the Indian sector of the Southern Ocean during the December to April time period. A noticeable decrease of the iceberg concentration during the warm period of the year has also been reported by Tournadre and others (2012, 2016) and Romanov and Romanova (2003, 2005).

CONCLUSION

Using over 60 000 ship observation reports of the iceberg concentration collected since the end of the 1940s we have produced a spatially detailed map characterizing the iceberg distribution around the Antarctic continent.

Table 4. Total area (in km²) and total volume (in km³) of icebergs of different shapes in the Southern Ocean by sector and latitude zone

Latitude	Tabular	Domed	Pyramidal	Sloping	Weathered	All shapes
Pacific sector (150° E–60° W)						
Area, km ²						
54°–66° S	2007	64	4	31	141	2247
66°–78° S	20 792	2735	78	378	506	24 450
54°–78° S	22 799	2798	82	409	647	26 736
54°–78° S	85.3%	10.5%	0.3%	1.5%	2.4%	100%
Volume, km ³						
54°–66° S	526	23	2	9	25	586
66°–78° S	6106	1198	38	96	86	7525
54°–78° S	6632	12 212	41	106	111	8111
54°–78° S	81.7%	15.1%	0.5%	1.3%	1.4%	100%
Atlantic sector (60° W–30° E)						
Area, km ²						
46°–66° S	5395	126	15	84	437	6057
66°–78° S	7958	855	24	115	197	9149
46°–78° S	13 353	981	39	199	634	15 206
46°–78° S	87.8%	6.4%	0.3%	1.3%	4.2%	100%
Volume, km ³						
46°–66° S	1414	46	7	25	78	1570.5
66°–78° S	2342	375	12	31	34	2794
46°–78° S	3757	421	19	56	111	4364
46°–78° S	86.1%	9.6%	0.4%	1.3%	2.6%	100%
Indian ocean sector (30° W–150° W)						
Area, km ²						
46°–66° S	7479	95	16	57	34	7992
66°–74° S	7485	228	17	16	125	7871
46°–74° S	14 965	324	33	73	469	15 864
46°–74° S	94.3%	2.0%	0.3%	0.5%	2.9%	100%
Volume, km ³						
46°–66° S	1961	35	8	17	61	2081
66°–74° S	2203	100	8	4	21	2337
46°–74° S	4164	135	16	21	82	4418
46°–74° S	94.2%	3.0%	0.4%	0.5%	1.9%	100%
Southern Ocean (180°W–180°E)						
Area, km ²						
46°–66° S	14 882	285	35	172	922	16 296
66°–78° S	36 235	3818	119	509	828	41 509
46°–78° S	51 117	4103	154	681	1750	57 805
46°–78° S	88.4%	7.1%	0.3%	1.2%	3.0%	100%
Volume, km ³						
46°–66° S	3901	104	17	51	164	4237
66°–78° S	10 652	1673	59	132	141	12 657
46°–78° S	14 553	1777	76	183	305	16 894
46°–78° S	86.1%	10.5%	0.5%	1.1%	1.8%	100%

Complementary to the mean iceberg concentration are maps of statistical characteristics of Antarctic icebergs including their variance, minimum and maximum concentration and the probability of the iceberg-free ocean. The derived iceberg distribution in the Southern Ocean along with statistical information on the iceberg shape and size have been used to estimate the total area and the total volume of ice in the Antarctic icebergs. Since most observations incorporated in the dataset were made from December to April, the results characterize the mean state of the Antarctic icebergs distribution during the warm period of the year.

Key features in the distribution of Antarctic icebergs established within this study were found to be in a good agreement with the location of calving sources and peculiarities of atmospheric and oceanic circulation in the region. The mean concentration of icebergs within the area in the Southern Ocean covered with observations amounted to eight icebergs per circle of 15 nm radius (equal to ~2400 km²). We estimated the instantaneous total number of icebergs in the Southern

Ocean at 132 269 with the uncertainty of ~7% of the value. The area and the total volume ice in all icebergs were found to be equal to 57 805 km² and 16 893 km³, respectively. Uncertainties associated with these latter estimates amounted to ~30%. Our estimates of the total number and volume of Antarctic icebergs were generally within the range of values obtained by other authors; however, the estimated total volume of ice in Antarctic icebergs was mostly larger than earlier estimates.

In our calculations, we have used a number of new approaches and techniques. Missing information on the iceberg concentration in a number of coastal areas have been replaced with data estimated from the relationship between the iceberg concentration and the productivity of close-by glaciers. Our estimates of the total area and volume of icebergs incorporate information on the fraction of icebergs of different shapes as well as on their geometrical properties and account for spatial variations of these parameters in the Southern Ocean. We believe that our estimates

have more sound physical justification than earlier estimates, are based on a larger observation dataset covering practically the entire Southern Ocean and therefore at this time can be considered as more accurate and reliable.

Nevertheless, it should be recognized that even with all improvements, the obtained estimates of the iceberg area-integrated characteristics (iceberg count, area and volume) are associated with substantial uncertainty and therefore should be considered only as a certain step closer to more reliable results. Obtaining more accurate estimates requires comprehensive observations of the iceberg concentration both in the summer and in the winter season. Further iceberg morphological observations are needed focusing on the iceberg length, height, area and shape. Better information on the draft of icebergs of different shapes would also help to better estimate the iceberg volume.

It also should be recognized that it is hard to expect a substantial increase in the number or frequency of ship observations of icebergs in the nearest future. Therefore it appears that further improvement in the characterization of the Antarctic iceberg number, distribution, size and volume will be associated mostly with the improvement of satellite-based remote-sensing instruments and techniques. The latter particularly concerns active microwave measurements capable of providing year-round, all-weather iceberg observations at high spatial resolution. Ship-based observations will still constitute an important element of the Antarctic iceberg monitoring system providing both additional information on the iceberg properties and ground truth for validation of remote-sensing retrievals.

SUPPLEMENTARY MATERIAL

The supplementary material for this article can be found at <https://doi.org/10.1017/aog.2017.2>

ACKNOWLEDGEMENTS

We thank two anonymous reviewers and Dr. Bob McNabb of University of Oslo for their thoughtful and detailed comments that helped us to substantially improve the paper.

REFERENCES

- Ardhuin F, Tournadre J, Queffelec P, Girard-Ardhuin F and Collard F (2011) Observation and parameterization of small icebergs: drifting breakwaters in the Southern Ocean. *Ocean Model.*, **39**, 405–410.
- Arrigo KR and van Dijken GL (2003) Impact of iceberg C-19 on Ross Sea primary production. *Geophys. Res. Lett.*, **30**(16). doi: 10.1029/2003GL017721.
- Ballantyne J (2002) A multidecadal study of the number of Antarctic icebergs using scatterometer Data, Brigham Young University online report <http://www.mers.byu.edu/long/paper/conf/IGARSS/>.
- Ballantyne J and Long DG (2002) A multidecadal study of the number of Antarctic icebergs using scatterometer Data. In *Proceedings of International Geoscience and Remote Sensing Symposium (IGARSS)*, 24–28 June 2002, Toronto, Canada, 1977–1979.
- Bigg GR, Wadley MR, Stevens DP and Johnson JA (1997) Modeling the dynamics and thermodynamics of icebergs. *Cold Reg. Sci. Technol.*, **26**, 113–135.
- Borodachev VE, Gavrilov VP and Kazanskii MM (1994) *Slovar' morskikh ledovykh terminov*. Hydrometeoizdat, St. Petersburg, 126 p. (Sea ice term glossary).
- Buinitskii VH (1973) *Morskije l'dy i aisbergi Antarktiki*, Izdatel'stvo Leningradskogo Gosudarstvennogo Universiteta. USSR, Leningrad, 255 p. (Sea Ice and Icebergs of Antarctic).
- Burrow CJ (2005) Icebergs near New Zealand and related phenomena. *N Z Nat. Sci.*, **30**, 57–64.
- Burrows CJ (1976) Icebergs in the Southern Ocean. *New Zealand Geographer*, **32**, 127–135.
- Dencausse G, Arhan M and Speich S (1989) Routes of Agulhas ring in the Southeast Cape Basin. *Deep Sea Res., Part 1*, **57**, 1406–1421.
- Depoorter MA and 6 others (2013). Calving fluxes and basal melt rates of Antarctic ice shelves. *Nature*, **502**(7469), 89–92.
- Dmitrash ZA (1973) O gorizontaľnyh razmerah antarkticheskikh aizbergov po dannym aerofotos'emki. *Info. Bull. Sovetskoi Antarkticheskoi Expedicii*, **86**, 40–41 (Horizontal dimensions of Antarctic Icebergs according to aerial photo-survey data).
- Dowdeswell JA and Bamber JL (2007) Keel depths of modern Antarctic icebergs and implication for sea-floor scouring in the geological records. *Marine Geol.*, **243**, 120–131.
- Dowdeswell JA, Whittington RJ and Hodgkins R (1992) The sizes, frequencies, and freeboards of the East Greenland icebergs observed using ship radar and sextant. *J. Geophys. Res.*, **97**(C), 3515–3528.
- Fricker HA, Young NW, Allison I and Coleman R. (2002). Iceberg calving from the Amery ice shelf, East Antarctica. *Ann. Glaciol.*, **34**(1), 241–246.
- Gladstone RM, Bigg GR and Nicholls KW (2001) Iceberg Trajectory Modelling and Meltwater Injection in the Southern Ocean. *Journal of Geophysical Research*, **106**(C9), 19,901–19,915.
- Gladstone RM and Bigg GR (2002) Satellite tracking of icebergs in the Weddell Sea. *Antarct. Sci.*, **14**, 278–287. doi: 10.1017/SO954102002000032.
- Gutt J and Starmang A (2001) Quantification of iceberg impact and benthic recolonisation patterns in the Weddell Sea (Antarctica). *Polar Biol.*, **24**, 615–619.
- Houghton J, Meira Filho L, Callander B, Harris N, Kattenberg A and Maskell K (eds) (1996) *IPCC climate change*. The IPCC Second Assessment Report. Cambridge University Press, New York.
- Jacka TH and Giles AB (2007) Antarctic iceberg distribution and dissolution from ship-based observations. *J. Glaciol.*, **53**, 341–350.
- Jacobs SS, Helmer H, Doake SCM, Jenkins A and Frolich R (1992) Melting of Ice Shelves and mass balance of Antarctica. *J. Glaciol.*, **38**, 375–387.
- Koshlyakov MN, Belkin IM, Radikevich VM and Romanov YA (1993) Icebergs along 67 S in the Pacific sector of the Antarctic in February–March of 1992. *Oceanology*, **33**, 720–727.
- Losev LS (1982) *Antarkticheskii ledovyi pokrov*. Science, Moscow, 157 p. (Antarctic Ice Cover).
- Lisitzin AP (2012) *Sea-Ice and Iceberg Sedimentation in the Ocean: Recent and Past*. Springer Science & Business Media, 563p.
- Massom RA (2003) Recent iceberg calving events in the Ninnis Glacier region, East Antarctic. *Antarct. Sci.*, **15**, 303–313.
- Matsumoto K (1996) An iceberg drift and decay model to compute the ice-rafted debris and iceberg meltwater flux: application to the interglacial North Atlantic. *Paleoceanography*, **11**, 729–742.
- McCartney MS and Donohue KA (2007) A deep cyclonic gyre in the Australian–Antarctic Basin. *Prog. Oceanogr.*, **75**, 675–750.
- Nazarov VS (1962) *Led Antarkticheskikh vod, Resultaty Mejdunarodnogo Geofyicheskogo Goda, Akademija Nauk SSSR. Sovetskii Geofyicheskii Komitet. Okeanologiya*, **6**, p. 72. (Ice of Antarctic Waters).
- Nigro MA and Cossano MA (2014) Identification of surface wind patterns over the Ross Ice Shelf, Antarctica using the self-organizing maps. *Monthly Weather Rev.*, **142**, 2361–2378.
- Orheim O (1980) Physical characteristics and life expectancy of tabular Antarctic icebergs. *Ann. Glaciol.*, **1**, 11–18.
- Orheim O (1985) Iceberg discharge and the mass balance of Antarctica, in *Glaciers Ice Sheets and Sea Level: Effect of a CO₂-induced Climatic Change*. In *Report of a Workshop held in Seattle, Washington*, 13–15 September 1984, 210–215. Nat. Acad. Press, Washington, DC.

- Orheim O (1990) Extracting climatic information from the observation of icebergs in the Southern Ocean (abstract). *Ann. Glaciol.*, **14**, 352.
- Orsi A and Ryan U (2001) Locations of the various fronts in the Southern Ocean. Australian Antarctic Data Centre—CAASM Metadata <http://data.aad.gov.au/aadc/metadata/>.
- Orheim O (2015) Oceanographic and glacier information from observations of 330 000 Antarctic icebergs. In *Presentation at 2015 Norwegian Geophysical Society Symposium*, 21–22 October 2015, Solstrand, Norway http://www.ngfweb.no/docs/ngf2015_foredrag_06_orheim.pdf.
- Popov LK and Voevodin VA (1996) *Aisbergi Mirovogo okeana*. Hydrometeoizdat, St. Peterburg, Russia, 138–141 (Icebergs of global ocean).
- Provorkin AV (1996) Gigantskie aisbergi Antarktidiy. In Popov LK and Voevodin VA eds. *Aisbergi Mirovogo okeana*. Hydrometeoizdat, St. Peterburg, Russia, 133–137. (Giant Icebergs of Antarctic).
- Rackow T, Wesche C, Timmermann R and Juricke S (2013) Modelling Southern Ocean iceberg drift and decay with FESOM-IB. In European Geophysical Union, 7 April 2013–12 April 2013, Vienna, Austria. <http://epic.awi.de/37482/>.
- Rackow T and 5 others (2017) A simulation of small to giant Antarctic iceberg evolution: differential impact on climatology estimates. *J. Geophys. Res. – Oceans*, **122**, 3170–3190.
- Radikevich VM and Romanov YA (1995) Using observations of iceberg drift for determining currents in the Pacific sector of the Southern Ocean. *Oceanology*, **35**, 130–139.
- Reeves S, Stuart K and Lamber B (2009) The Antarctic Iceberg Tracking Database <http://www.scp.dyu.edu/data/iceberg/database>.
- Rignot E, Jackobs S, Mouginot J and Scheuchl B (2013) Ice Shelf melting around Antarctica. *Science*, **341**, 266–270. doi: 10.1126/science.1235798.
- Romanov AA (1996a) Novye dannye o raspredelenii, kolichestve i ob'eme Antarkticheskikh aisbergov. In Popov LK and Voevodin VA eds. *Aisbergi Mirovogo okeana*. Hydrometeoizdat, St. Peterburg, Russia, 120–127 (New data on the Distribution, Amount and Volume of the Antarctic icebergs).
- Romanov AA (1996b) Ice Navigation Condition in the Southern Ocean, Tech. Doc., WMO/TD, 783, 119. World Meteorological Organization, Geneva, Switzerland.
- Romanov YA and Korotkov AI (2001) Seasonal variations in Iceberg Abundance in Eastern Antarctica (50°–70° N, 0°–120° E), Doklady Earth Science. *Geography*, **379**, 611–614.
- Romanov YA and Romanova NA (2003) Concentration of icebergs in the Atlantic sector of the Antarctic region, Doklady Earth Science. *Geography*, **393**, 1146–1150.
- Romanov YA and Romanova NA (2005) Icebergs in the Australian Sector of Antarctic region, Doklady Earth Science. *Geography*, **402**, 649–651.
- Romanov YA, Romanova NA and Romanov P (2008) Distribution of icebergs in the Atlantic and Indian ocean sectors of the Antarctic region and its possible links with ENSO. *Geophys. Res. Lett.*, **35**, L02506. doi:10.1029/2007GL031685.2008.
- Romanov YA, Romanova NA and Romanov P (2012) Shape and size of Antarctic icebergs derived from ship observation data. *Antarct. Sci.*, **24**, 77–87.
- Romanov YA, Romanova NA and Romanov P (2014) Changing effect of El Niño on Antarctic iceberg distribution: from canonical El Niño to El Niño Modoki, *J. Geophys. Res. Oceans*, **119**, 595–614. doi: 10.1002/2013JC009429.
- Schell II (1974) *Oceanographic Encyclopedia. Icebergs*. Hydrometeoizdat, Leningrad, Russia, 12–14.
- Schodlok MP, Hellmer HH, Rohardt G and Fahrbach E (2006) Weddell Sea iceberg drift: five year of observations. *J. Geophys. Res.*, **111**, C06018. doi: 10.1029/2004JC002661.
- Schwarz JN and Schodlok MP (2009) Impact of drifting icebergs on surface phytoplankton biomass in the Southern ocean: ocean colors remote sensing and in situ iceberg tracking. *Deep Sea Res., Part I*, **56**, 1727–1741. doi: 10.1016/j.dsr.2009.05.003.
- Shilnikov VI (1960) Ob'em i kolichestvo aizbergov v Antarktike. *Info. Bull. Sovetskoi Antarkticheskoi Ekspeditsii*, **21**, 34–37. (Volume and amount of icebergs in Antarctica).
- Shilnikov VI (1969) Aizbergi (Icebergs). In Tolstikov YI ed. *Atlas Antarktiki. Hydrometeoizdat*, Leningrad, Russia, v2, 455–465 (Atlas of Antarctic).
- Silva T, Bigg G and Nicholls K (2006) The contribution of giant icebergs to the Southern Ocean freshwater flux. *J. Geophys. Res.*, **111**, C09004. doi: 10.1029/2004JC002843.
- Smith KL (2011) Free-drifting icebergs in the Southern Ocean: an overview. *Deep Sea Res., Part II*, **58**, 1277–1284.
- Spandonide B (2012) Iceberg water transportation from Antarctic to Australia. (PhD thesis, University of Tasmania), 539p.
- Sprintall J, Chereskin TK and Sweency C (2012) High-resolution underway upper ocean and surface atmosphere observations in Drake Passage. *Oceanography*, **25**, 70–81.
- Tournadre J, Whitmer K and Girard-Ardhuin F (2008) Iceberg detection in open water by altimeter waveform analysis. *J. Geophys. Res.: Oceans*, **113**(C08040). Doi: 10.1029/2007JC004587.
- Tournadre J, Girard-Ardhuin F and Legresy B (2012) Antarctic iceberg distribution. 2002–2010. *J. Geophys. Res.*, **117**. doi: 10.1029/2011JC007441.
- Tournadre J, Bouhier N, Girard-Ardhuin F and Remi F (2015) Large icebergs characteristics from altimeter waveform analysis. *J. Geophys. Res.*, **120**, 1954–1974. Doi: 10.1002/2014JO10502.
- Tournadre J, Bouhier N, Girard-Ardhuin F and Remy F (2016) Antarctic iceberg distribution 1992–2014. *J. Geophys. Res.*, **121**, 327–349. doi: 10.1002/2015JC011178.
- Wadhams P (1988) Winter observations on iceberg frequencies and sizes in the South Atlantic Ocean. *J. Geophys. Res.*, **93**(C4), 3583–3590.
- Weeks WF and Campbell WJ (1973) Icebergs as a fresh-water source: an appraisal. *J. Glaciol.*, **12**, 207–233.
- Wesche C and Dierking W (2015) Near-coastal circum-Antarctic iceberg size distributions determined from synthetic Aperture Radar Images. *Remote Sens. Environ.*, **156**, 561–569.
- Wesche C, Jansen D and Dierking W (2013) Calving fronts of Antarctica: mapping and classification. *Remote Sens.*, **5**, 6305–6322. doi: 10.3390/rs5126305.
- Williams RN, Rees G and Young NW (1999) A technique for the identification and analysis of icebergs in synthetic aperture radar images of Antarctica. *Int. J. Remote Sens.*, **20**, 3183–3199.
- Williams RS and Ferrigno JV (1988) Satellite Image Atlas, U.S. Geological Survey, Professional Paper 1386-B, U.S. Gov. Printing. Office, Washington, 288p.
- WMO (1970) Sea-ice nomenclature, terminology, codes and illustrated glossary. MO/OMM/BMO. World Meteorological Organization, Geneva, 145 p.
- Young NW, Turner D, Hyland G and Williams RN (1998) Near-coastal iceberg distributions in east Antarctica. *Ann. Glaciol.*, **27**, 68–74.